NIH Public Access
Author Manuscript
Neuron. Author manuscript; available in PMC 2014 March 20.

Published in final edited form as:
Neuron. 2013 March 20; 77(6): 1055–1068. doi:10.1016/j.neuron.2013.01.015.

Etv1 Inactivation Reveals Proprioceptor Subclasses that Reflect the Level of NT3 Expression in Muscle Targets

Joriene C. de Nooij[1,2], **Staceyann Doobar**[1,2], and **Thomas M. Jessell**[1,2,*]

[1]Department of Neuroscience, Howard Hughes Medical Institute, Kavli Institute for Brain Science, Columbia University, New York, NY 10032, USA

[2]Department of Biochemistry and Molecular Biophysics, Howard Hughes Medical Institute, Kavli Institute for Brain Science, Columbia University, New York, NY 10032, USA

SUMMARY

The organization of spinal reflex circuits relies on the specification of distinct classes of proprioceptive sensory neurons (pSN), but the factors that drive such diversity remain unclear. We report here that pSNs supplying distinct skeletal muscles differ in their dependence on the ETS transcription factor Etv1 for their survival and differentiation. The status of Etv1-dependence is linked to the location of proprioceptor muscle targets: pSNs innervating hypaxial and axial muscles depend critically on Etv1 for survival, whereas those innervating certain limb muscles are resistant to Etv1 inactivation. The level of NT3 expression in individual muscles correlates with Etv1-dependence and the loss of pSNs triggered by *Etv1* inactivation can be prevented by elevating the level of muscle-derived NT3—revealing a TrkC-activated Etv1-bypass pathway. Our findings support a model in which the specification of aspects of pSN subtype character is controlled by variation in the level of muscle NT3 expression and signaling.

INTRODUCTION

Proprioceptive sensory neurons serve a key role in refining the output of the spinal motor system through the provision of feedback signals that convey the state of muscle activity to motor neurons (Pierrot-Deseilligny and Burke, 2005; Windhorst, 2007). The basic wiring of sensory-motor reflex circuits has been argued to form in a manner that is independent of patterned neural activity (Mendelson and Frank, 1991), implying that molecular distinctions in sensory and motor neuron identity direct the selectivity of these circuits.

Spinal motor neurons can be subdivided into discrete functional classes, the molecular identities and settling positions of which are aligned with the location of their skeletal muscle targets (Romanes, 1951; Demireva et al., 2011). Axial, hypaxial, and limb muscles occupy different peripheral domains and are innervated by topographically segregated motor columns (Jessell et al., 2011). Individual limb muscles are innervated by clustered and stereotypically positioned motor neuron pools (Landmesser, 1978; Demireva et al., 2011; Levine et al., 2012). Moreover, each muscle contains extrafusal and intrafusal myofibers that are innervated, respectively, by the alpha and gamma motor neurons that populate each motor pool (Kanning et al., 2010). These modular features of motor neuron subtype are

©2013 Elsevier Inc.

*Correspondence: tmj1@columbia.edu.

SUPPLEMENTAL INFORMATION

Supplemental Information includes seven figures, three tables, and Supplemental Experimental Procedures and can be found with this article online at http://dx.doi.org/10.1016/j.neuron.2013.01.015.

NIH-PA Author Manuscript
NIH-PA Author Manuscript
NIH-PA Author Manuscript

NIH-PA Author Manuscript

NIH-PA Author Manuscript

NIH-PA Author Manuscript

specified by transcriptional determinants, notably members of the Homeodomain and ETS families and their downstream effector targets (Dasen and Jessell, 2009).

Less is known of the way in which proprioceptor subtype identities are established, even though such distinctions direct the fine pattern of sensory-motor connectivity. The modular assignment of motor neurons into α/γ, pool, and columnar subclasses poses the question of whether proprioceptive sensory neuron (pSN) diversification adheres to a similar organizational scheme. Certain anatomical observations support this view. Within individual muscles, pSNs project to one of two distinct transduction systems–muscle spindles (MSs) and Golgi tendon organs (GTOs) (Figure 1A; Matthews, 1972). pSNs innervating MSs and GTOs pursue distinct intraspinal axonal trajectories and terminate at different dorsoventral positions (Brown, 1981; Chen et al., 2006). Moreover, pSNs that supply individual MSs form selective connections with motor neurons in pools that project to the same or functionally-related muscles (Eccles et al., 1957; Mears and Frank, 1997), implying that pSNs also possess muscle-specific ("pool") identities. At a broader organizational level, pSNs innervating axial, hypaxial, and limb muscles can be distinguished by their projection to, and connections with, neurons in different motor columns (Vanderhorst and Holstege, 1997; Nakayama et al., 1998).

Transcription factors also control early steps in the specification of proprioceptors. The bHLH protein Neurogenin 2 and the POU protein Brn3 act as determinants that direct sensory neural progenitors toward a proprioceptor fate (Xiang et al., 1997; Ma et al., 1999). The neuronal context conferred by these two factors results in activation of expression of the transcription factor Runx3 (Rx3), consolidating pSN identity (Kramer et al., 2006; Dykes et al., 2011). Ectopic expression of Rx3 in cutaneous sensory neurons is sufficient to divert their dorsally targeted axons to locations deep in the ventral spinal cord, a defining feature of MS-innervating proprioceptors (Chen et al., 2006). Conversely, RNAi-mediated reduction in Rx3 expression causes the axons of pSNs to terminate in the intermediate rather than ventral domain of the spinal cord. These findings suggest that graded Rx3 activity controls the dorsoventral distinction in termination zones of MS and GTO-innervating proprioceptors (Chen et al., 2006).

The early survival of proprioceptors requires exposure to neurotrophin 3 (NT3) and activation of the tyrosine kinase receptor TrkC (Klein et al., 1994; Fariñas et al., 1994). In addition, NT3/TrkC signaling induces pSN expression of Etv1 (Er81), an ETS class transcription factor (Arber et al., 2000; Patel et al., 2003). Genetic inactivation of Etv1 causes the axons of many pSNs to terminate in an ectopic dorsal position within the intermediate spinal cord (Arber et al., 2000). The precise role of Etv1 in proprioceptor differentiation has not been resolved, however. Here we show that Etv1 has a fundamental role in promoting the survival and differentiation of a subset of pSNs. The status of Etv1-dependence varies with muscle target: pSNs innervating hypaxial and axial muscles exhibit an almost complete dependence on Etv1 for survival, whereas those innervating hindlimb muscles exhibit a mosaic, muscle-by-muscle, sensitivity or resistance to Etv1 inactivation. Strikingly, the level of NT3 expression in individual muscles predicts the Etv1-dependence of pSNs. Thus, critical aspects of pSN subtype character and connectivity appear to be controlled by muscle-by-muscle variation in the strength of NT3 expression and signaling.

RESULTS

Proprioceptor Identification Depends on Coincident Marker Expression

To assess the role of Etv1 in the differentiation of proprioceptor subtypes we sought molecular markers that provide unambiguous identification of pSNs in embryonic (e) and postnatal (p) lumbar dorsal root ganglia (DRG).

NIH-PA Author Manuscript

NIH-PA Author Manuscript

NIH-PA Author Manuscript

We analyzed expression of the cell surface receptor TrkC, the transcription factor Rx3, and the cytoplasmic Ca^{2+} binding protein Parvalbumin (Pv)–markers previously linked to pSN identity (Arber et al., 2000; Lallemend and Ernfors, 2012). All Rx3 neurons and ~90% of Pv neurons expressed TrkC, whereas ~40% – 50% of TrkC neurons lacked expression of Rx3 and/or Pv (Figures 1B–1F). In addition, ~85% of Rx3 neurons expressed Pv, and ~90% of Pv^+ DRG neurons expressed Rx3 (Figures 1D–1F and Figure S1 available online; Table S1). Thus, the composite expression of TrkC, Rx3, and Pv defines four neuronal subsets: two large populations of $TrkC^+Rx3^{off}Pv^{off}$ and $TrkC^+Rx3^+Pv^+$ neurons, and two small subsets of $TrkC^+Rx3^+Pv^{off}$ and $TrkC^{off}Rx3^{off}Pv^+$ DRG neurons. In marked contrast to the profile of endogenous TrkC expression, analysis of a *TrkC:GFP* BAC transgenic line (Gong et al., 2003) revealed GFP expression only in $TrkC^+Rx3^+Pv^+$ and $TrkC^+Rx3^+Pv^{off}$ neurons (Figures 1G, 1H, and S2), a restriction we use in studies described below.

Which of these subsets represent pSNs? Many $TrkC^+Rx3^{off}Pv^{off}$ neurons expressed Ret, TrkB, and/or TrkA (Figure S2, data not shown), indicating that expression of TrkC in the absence of Rx3 or Pv marks cutaneous sensory neurons. To determine the sensory modalities associated with the remaining three neuronal populations we compared cell body marker status and axonal projection pattern in transgenic mice carrying reporter genes directed by tamoxifen-activated *Rx3:Cre*^{ER} or *Pv:Cre* driver alleles (see Table S2 for mice used in this study). Bicistronic mGFP/nuclear LacZ (nLZ), or tdTomato (tdT) reporters were used to label $Rx3^+$ or Pv^+ sensory neuron cell bodies, along with their central and peripheral axons (Figures 1I, 1J, S1, and S3) (Hippenmeyer et al., 2005; Madisen et al., 2010).

In *Rx3:Cre*^{ER}-directed mGFP-nLZ reporter crosses we found that all $mGFP^+$ DRG neurons expressed nuclear Rx3 protein (Figure S3). Only ~10% of all $Rx3^+$ neurons expressed mGFP, presumably a reflection of the inefficiency of tamoxifen-triggered Cre recombination of target genes in DRG neurons (Zhao et al., 2006). Nevertheless, *Rx3:Cre*^{ER}-directed mGFP reporter expression was observed in both MS and GTO pSN sensory endings in limb, axial and hypaxial muscles (Figure 1I; data not shown). *Pv:Cre*-directed reporter expression was restricted to Pv^+ neurons and was detected in ~98% of DRG neurons that expressed endogenous Pv (Figure S1). mGFP-labeled axons innervated virtually all MSs and GTOs in axial, hypaxial, and hindlimb muscles (Figures 1J and S1). These data, together with the fact that all MS- and GTO-innervating pSNs are eliminated in *TrkC* and *Rx3* mutant mice (Klein et al., 1994; Kramer et al., 2006; J.C.d.N. and T.M.J., unpublished data) suggest that the larger $TrkC^+Rx3^+Pv^+$ neuronal population represents authentic pSNs.

We next examined the profile of Etv1 expression with reference to the $TrkC^+Rx3^+Pv^+$ pSN population. At neonatal stages, Etv1 expression was detected in all $TrkC^+Rx3^+Pv^+$ neurons (Figures 1D–1F). Nevertheless, ~60% of $Etv1^+$ neurons lacked Rx3 and/or Pv expression, indicative of sensory neuron classes other than proprioceptors (Figure S2). In addition, Etv1 was observed in ~60% of $Rx3^{off}Pv^+$ neurons, but was excluded from $Rx3^+Pv^{off}$ neurons (Figure 1D, data not shown). Thus, all proprioceptors express Etv1, but its expression is not restricted to pSNs.

Analysis of the pattern of reporter expression directed by *Rx3:Cre*^{ER} and *Pv:Cre* driver lines also provided insight into the identities of the two smaller $TrkC^+Rx3^+Pv^{off}$ and $TrkC^{off}Rx3^{off}Pv^+$ sensory neuronal subsets. *Pv:Cre* directed mGFP-labeled axons were found as Lanceolate endings and also innervated Meissner and Pacinian corpuscles (Figure S1). In *Rx3:Cre*^{ER} reporter crosses, mGFP-labeled axons contacted Merkel cells rather than Lanceolates or Meissner corpuscles (Figure S3). Thus, $Rx3^+Pv^{off}$ and $Rx3^{off}Pv^+$ subclasses represent distinct sets of low-threshold cutaneous mechanoreceptors (Figure 1K).

NIH-PA Author Manuscript

NIH-PA Author Manuscript

NIH-PA Author Manuscript

Together, these findings indicate that TrkC, Rx3, Pv, and Etv1, individually, fail to serve as reliable markers of pSNs in mouse lumbar DRG. Nevertheless, coincident pairings of Rx3 with Pv, of Rx3 with Etv1, and of *TrkC:GFP* with Etv1, do mark proprioceptors with high specificity (Figure 1K). In subsequent analyses we have relied on one or more of these molecular pairings to mark pSNs.

Proprioceptor Diversity Uncovered by Differential Etv1-Dependence

To address the role of Etv1 in the differentiation of proprioceptor subclasses we examined pSN phenotypes in *Etv1* mutant mice. We used two *Etv1* mutant alleles, both phenotypic nulls (together termed $Etv1^{-/-}$) (Arber et al., 2000). $Etv1^{ETS}$ lacks the ETS domain whereas $Etv1^{nLZ}$ lacks the transcriptional activation domain. Analysis of $Etv1^{nLZ}$ mice permitted us to identify mutant pSNs through *nLZ* reporter expression. We routinely analyzed *Etv1* mutant phenotypes in mice carrying the *TrkC:GFP* transgene to restrict our analysis to pSNs. We also compared the impact of Etv1 inactivation in rostral lumbar (L2) DRG, which contain pSNs with peripheral axons that supply predominantly axial and hypaxial muscles, with that in caudal lumbar (L5) DRG, where most pSNs innervate limb muscles (Figure 2A) (Molander and Grant, 1986; Iscoe, 2000; our unpublished observations).

In $Etv1^{-/-}$;*TrkC:GFP* mutants the number of pSNs was reduced significantly. At L2 levels, the number of $Rx3^+$ neurons detected at e14.5, soon after the onset of Etv1 expression, was reduced by ~30%, and by p0 and p10 we detected an ~80% loss of pSNs (nLZ^+TrkC:GFP^+ or nLZ^+Rx3^+) (Figures 2B, 2C, S4; Table S1). In contrast, pSN number at L5 levels was reduced by only ~40% at p0 and p10 (Figures 2B, 2C; Table S1;data not shown). Thus, the extent of loss of pSNs differs markedly in rostral and caudal lumbar DRG. To resolve whether this loss reflects the absence of pSN marker expression or neuronal death, we analyzed pSN differentiation after inactivating both *Etv1* and the pro-apoptotic gene *Bax1* (White et al., 1998; Patel et al., 2003). Analysis of the number of pSNs ($Rx3^+nLZ^+$) in $Bax1^{-/-}$ single mutant as well as $Etv1^{-/-}$;$Bax1^{-/-}$ mutant mice at p0 revealed a >2-fold increase when compared with wild-type mice (Figures 2D, 2E, and S4; White et al., 1998). Thus, inactivation of Etv1 results in overt neuronal loss, indicating an essential survival function for Etv1 in subsets of pSNs.

Blocking sensory neuron death through Bax1 inactivation also permitted us to examine whether the loss of Etv1 impacts other aspects of pSN differentiation. We compared pSN cell body diameter in wild-type, $Bax1^{-/-}$, and $Etv1^{-/-}$; $Bax1^{-/-}$mice. In $Bax1^{-/-}$ mutants, >80% of $Etv1^{nLZ+}$TrkC:GFP^+ pSNs in rostral lumbar DRG fell within the wild-type range (17–30 μm in diameter), with the remaining ~20% possessing smaller somatic diameters (10–16 μm) (Figures 2Dii and S4). In contrast in $Etv1^{-/-}$; $Bax1^{-/-}$ mice, only ~30% of $Etv1^{nLZ+}$TrkC:GFP^+ pSNs neurons fell within the wild-type range, and ~70% possessed smaller diameters (Figures 2Diii and S4). Thus, Etv1 promotes aspects of pSN differentiation in addition to its role in neuronal survival.

We also examined whether Etv1 regulates pSN survival and differentiation in a cell-autonomous manner. To assess this, we crossed a DRG-restricted *Ht-PA:Cre* driver line with a conditional $Etv1^{flx}$ mutant allele, deleting Etv1 expression from sensory neurons while preserving expression in intrafusal fibers within muscle spindles (Pietri et al., 2003; Patel et al., 2003; Hippenmeyer et al., 2002). Inactivation of Etv1 in sensory neurons led to an ~65%–70% reduction in the number of $Rx3^+$ DRG neurons at L2 levels, a value close to the loss in constitutive *Etv1* mutants (Figures 2F and 2G). Thus, Etv1 expression and activity appears to be required autonomously for the embryonic differentiation and survival of a subset of pSNs (Figure 2H).

NIH-PA Author Manuscript

NIH-PA Author Manuscript

NIH-PA Author Manuscript

pSN Etv1-Dependence Does Not Segregate with MS Subclass Identity

We considered whether rostrocaudal positional differences in the Etv1-dependence of pSNs might reflect heightened Etv1 sensitivity of the subset of sensory neurons that innervate MSs (Figure 1A). This possibility emerged from our observation that in *Etv1* mutants 80% of pSNs in L2 ganglia are lost, coupled with the fact that the major targets of L2 pSNs–axial and hypaxial muscles–contain many MSs but few GTOs (Figure S1; J.C.d.N. and T.M.J., unpublished data). In this view, the more modest 40%, reduction of pSNs in L5 DRG that is detected in *Etv1* mutants matches the fact that their limb muscles contain proportionally fewer MSs and more GTOs (Figure S1) (Banks et al., 2009).

To resolve if MS-innervating pSNs are eliminated preferentially after inactivation of Etv1, we devised a genetic strategy to label, selectively, the subset of pSNs that innervate MSs. We used a3.2 kb human *Egr3* promoter fragment to direct wheat germ agglutinin (WGA) expression to the intrafusal muscle fibers of MSs (Tourtellotte and Milbrandt, 1998; Yoshihara, 2002). We reasoned that localized WGA secretion from MSs would result in selective uptake of this lectin tracer into MS-associated sensory endings, and subsequently, via retrograde transport, accumulation in neuronal cell bodies in DRG (Figures 3A, 3B, and S5).

After introducing the *Egr3:WGA* allele into $Etv1^{nLZ/+}$ mice, we found WGA accumulation in ~70% of $Rx3^{+}Etv1^{nLZ+}$ pSNs in L2 DRG, and ~55% in L5 DRG accumulated WGA (Figures 3C, 3D; Table S3). These findings imply that MS-innervating pSNs are somewhat more prevalent in L2 than L5 DRG. More critically, in *Etv1* mutants, ~20% of the normal number of WGA^{+} pSNs were preserved, indicating that there is not a selective loss of MS-innervating pSNs. Moreover, we found that the decrease in WGA-labeled pSNs in *Etv1* mutants reflects, in large part, a ~65% loss in the number of MSs that express WGA in *Etv1* mutants (Figure 3E). Together, these data argue against a stringent segregation of Etv1-dependence with MS-innervating pSNs.

Proprioceptor Loss in *Etv1* Mutant Mice Segregates with Muscle Target

We asked if pSN sensitivity to Etv1 deprivation instead respects regional or muscle-specific organizational rules. To assess this issue, we compared the incidence of pSN sensory endings in axial, hypaxial and limb muscles in wild-type and *Etv1* mutants at neonatal stages. We focused primarily on the pattern of MS innervation because it was difficult to identify GTO-associated pSN endings reliably in *Etv1* mutants (see Figure S6). Spindle-associated sensory endings (SSEs) were visualized by vGluT1 expression (Wu et al., 2004). We also assessed the number of MSs by virtue of expression of *Etv4/PEA3*, an ETS factor induced in intrafusal muscle fibers by pSN axons (Hippenmeyer et al., 2002). Expression of *Etv4* in MSs was also monitored by βGalactosidase (βGal) labeling in $Etv4^{nLZ}$ transgenic mice (Arber et al., 2000). In *Etv1* mutants analyzed at p0–3 we found that hypaxial (body wall and intercostal) muscles lacked $vGluT1^{+}$ SSEs or $Etv4^{nLZ+}$ MSs (Figures 4A, 4C, and S7). Axial muscles retained ~3% of $vGluT1^{+}$ SSEs and ~14% of $Etv4^{nLZ+}$ MSs (Figures 4A and 4C). Thus pSNs innervating hypaxial, and to a somewhat lesser extent axial, muscles are sensitive to the loss of Etv1 activity.

In hindlimb muscles, however, sensory innervation of MSs in *Etv1* mutants was more significantly preserved. Within the limb as a whole, ~50% of all $vGluT1^{+}$ SSEs and $Etv4^{nLZ+}$ MSs persisted (Figure 4C). We observed a striking muscle-to-muscle variation in the status of pSN innervation. The soleus (Sol), gastrocnemius (G), extensor digitorum longus (EDL), peroneus brevis (PB), and quadriceps (Q; rectus femoris and vasti) muscles exhibited a near-normal incidence of $vGluT1^{+}$ SSEs and $Etv4^{nLZ+}$ MSs in *Etv1* mutants (Figures 4A–4D and S7). Nevertheless, the SSEs present in Sol or EDL muscles in *Etv1*

NIH-PA Author Manuscript

NIH-PA Author Manuscript

NIH-PA Author Manuscript

mutants exhibited disorganized annulospiral structures (Figure S6), revealing a function for Etv1 in later steps in the differentiation of pSNs. In contrast, the gluteus (Gl), biceps femoris (BF), and semitendinosus (St) muscles, exhibited an almost complete absence of SSEs and Etv4^{nLZ+} MSs (Figures 4B, 4D, and S7). The semimembranosus (Sm), plantaris (Pl), peroneus longus (PL), and tibialis anterior (TA) muscles exhibited partial (20%–60%) depletions in SSEs and Etv4^{nLZ+} MSs (Figures 4D and S7). To the extent possible, we found a clear concordance between the status of spindle and GTO innervation in *Etv1* mutant muscles.

Do pSN axons ever reach their normal muscle targets in *Etv1* mutants? To assess this, we examined when the defect in peripheral sensory projections becomes apparent in *Etv1* mutants, monitoring the presence of TrkC$^+$ and TrkC:GFP$^+$ pSN axons in muscle targets at e15.5. We focused this analysis on hypaxial and gluteus limb muscles because of the Etv1-dependence of pSNs innervating these muscles. We found that TrkC$^+$ and TrkC:GFP$^+$ pSN axons were detected in hypaxial and gluteus muscle in *Etv1* mutants (Figure 4E, data not shown). Despite the early intramuscular presence of pSN axons, muscle spindle differentiation was not initiated, as assessed by the lack of expression of *Etv4* in intrafusal fibers, and sensory endings were correspondingly disorganized (Figures 4 and S7). Thus, some Etv1-dependent pSNs initially reach their target muscles but are not capable of inducing MS differentiation.

Are distinctions in pSN Etv1-dependence also reflected in the intraspinal trajectory of pSN axons? To assess this, we traced the central projection of pSN axons at T9, L2, and L5 levels at p5–6 using rhodamine-dextran (RhD) dorsal root fills in wild-type and *Etv1* mutant mice and quantified the fraction of RhD-labeled pSN axons that pursued medial (presumed axial muscle-derived) and lateral (presumed hypaxial or limb muscle-derived) trajectories (Figures 5A and 5B). In wild-type mice at T9 levels, ~56% of the RhD-labeled pSN axonal population pursued a medial, and ~44% a lateral trajectory (Figure 5B). A similar distribution was observed at L2 levels: ~55% of the pSN axonal population projected medially and ~45% laterally. At L5 levels, ~22% of the pSN axonal population pursued a medial, and ~78% a lateral trajectory (Figure 5B). In contrast, in *Etv1* mutants, we detected an almost complete depletion in the laterally-targeted pSN axon fascicle at T9, L2, and L5 levels (~98% at T9, ~99% at L2, ~93% at L5; Figures 5B and 5C), a finding that extends previous observations (Li et al., 2006). At L5 levels the reduction in the density of laterally-targeted axons was more severe than predicted by the preservation of ~60% of L5 pSN neurons and ~50% of limb muscle SSEs. We also detected a drastic reduction in medially-oriented pSN axons at all segmental levels (~82% at T9, ~84% at L2, ~81% at L5; Figures 5B and 5C). Thus, the loss of intraspinal axons supplying axial and hypaxial muscle targets in *Etv1* mutants is in good agreement with the lack of SSEs in axial and hypaxial muscle targets, although limb-innervating pSN axons are more severely compromised than expected based on the preservation of limb muscle SSEs.

pSN Etv1-Dependence Correlates Inversely with Muscle Target NT3 Expression

We next examined whether the status of Etv1-dependence reflects differences in extrinsic signals that act upon developing pSNs. One plausible candidate for such an extrinsic signal is NT3, which serves as a critical survival and differentiation factor for pSNs and is required for induction of Etv1 expression (Fariñas et al., 1994, 1996; Patel et al., 2003).

We first assessed if variations in a local ganglionic source of NT3 underlies the rostrocaudal differences in Etv1-sensitivity, examining *NT3* expression by RNA in situ hybridization, as well as by expression of a βGal reporter expressed from the *NT3* locus (Fariñas et al., 1994). We detected a striking difference in the level of *NT3* expression in rostral and caudal lumbar DRG (Figure 6A). L2 DRG were virtually devoid of *NT3* or βGal expressing cells, whereas

NIH-PA Author Manuscript

NIH-PA Author Manuscript

NIH-PA Author Manuscript

many *NT3* and βGal expressing cells were observed in L4–L5 DRG (Figure 6A) (see also Fariñas et al., 1996). Here, βGal was expressed in Runx1^{+} (Rx1^{+}) cutaneous sensory neurons but not in Rx3^{+} pSNs (Figure 6B), suggestive of a paracrine role for NT3 in pSN differentiation. To examine the relevance of intraganglionic NT3 in setting the Etv1-dependence of pSNs, we eliminated expression of *NT3* from DRG cells selectively, using an *Ht-PA:Cre* driver and an *NT3^{flx}* allele (Pietri et al., 2003; Bates et al., 1999). Elimination of NT3 from DRG did not affect the number of pSNs in L5 DRG, nor did we observe a larger reduction in pSN survival in *Etv1$^{-/-}$; Ht-PA:Cre; NT3$^{flx/flx}$* L5 DRG when compared to *Etv1* mutants (Figure 6C, data not shown). Thus, intraganglionic NT3 expression alone appears not to underlie the L2/L5 distinction in pSN Etv1-dependence.

In the limb, NT3 is expressed by embryonic mesenchyme, as well as by skeletal extra- and intrafusal muscle fibers (Fariñas et al., 1996; Copray and Brouwer, 1994), prompting us to explore whether limb muscle *NT3* expression levels underlie the differences in pSN Etv1-dependence. We analyzed βGal activity levels in hindlimbs of e15.5 *NT3:lacZ* mice, and performed quantitative real time PCR (qRT-PCR) of *NT3* transcript expression. Histologically, βGal activity levels varied markedly between individual limb muscles. Muscles innervated by Etv1-dependent pSNs (gluteus, BF) exhibited lower levels of βGal activity than muscles innervated by Etv1-independent pSNs (soleus, EDL, RF) (Figure 6D).

To determine muscle NT3 expression levels more quantitatively, we performed qRT-PCR on embryonic (e15–16) body wall (BW), TA, and Sol muscles, selected because they spanned the spectrum of pSN Etv1-dependence. *NT3* expression levels were normalized to *MyoD*, a muscle-specific transcript expressed equally in all embryonic muscles (Hinterberger et al., 1991). We found that Sol muscle *NT3* levels were ~2-fold higher than in TA muscle, and that TA muscle showed a ~3-fold increase in *NT3* levels compared to BW muscle (Sol to TA, $p < 0.005$; Sol to BW, $p < 0.001$; TA to BW, $p = 0.014$, one-way ANOVA) (Figure 6E). Taken together, these data indicate that the extent of Etv1-dependence correlates inversely with muscle *NT3* expression level (Figure 6F).

Elevated Muscle NT3 Expression Compensates for the Loss of *Etv1* Activity

Do differences in muscle NT3 level underlie the differential Etv1-dependence of L2 and L5 pSNs? To test this, we examined the relationship between NT3 level and pSN Etv1-dependence in wild-type and *Etv1$^{-/-}$* mice, comparing L2 and L5 proprioceptor neuronal number under conditions of elevated or reduced muscle NT3 expression.

To elevate muscle NT3 expression, we took advantage of mice in which NT3 is overexpressed in skeletal muscle under the control of a myosin light chain (*mlc1*) promoter (Taylor et al., 2001). In wild-type mice, muscle-targeted expression of an *NT3* transgene resulted in a 2.3-fold increase in pSN number (from ~230 pSNs/DRG in wild-type mice to ~540 pSNs/DRG in *mlc1NT3* mice) (Figures 7A and 7B). In L5 DRG the number of pSNs increased by 1.4-fold (from ~550 in wild-type to ~810 pSNs/DRG in *mlc1NT3* mice) (Figures 7A and 7B). These NT3-mediated increases in pSN number in L2 and L5 DRG were quantitatively similar to increases observed in *Bax1$^{-/-}$* mice (Figure S4), consistent with the idea that enhanced NT3 signaling prevents the apoptotic death of pSNs. In *NT3* heterozygous mice the number of L2 pSNs was reduced by ~70% of wild-type values, but in L5 DRG the reduction was only ~55% (Figure 7C). Thus, the L2 pSN population is more sensitive to elevating or reducing peripheral NT3 levels than their L5 pSN counterparts.

We next examined how an elevation of muscle NT3 expression impacts L2 and L5 pSN number in *Etv1* mutants. Expression of the *mlc1NT3* transgene in *Etv1* mutants increased the number of L2 pSNs 2.1-fold, and the number of L5 pSNs 1.4-fold, elevations almost identical to those observed in wild-type mice (Figures 7A and 7B). In addition, muscle

NIH-PA Author Manuscript

NIH-PA Author Manuscript

NIH-PA Author Manuscript

expression of the *mlc1NT3* transgene largely restored intraspinal axonal trajectories of pSNs supplying axial, hypaxial, and limb muscles (Figure 5C; see also Li et al., 2006). More specifically, we determined whether elevation of *NT3* expression in *Etv1* mutants is able to restore pSN innervation of muscles that express low levels of *NT3*. Assessing the status of sensory innervation of body wall, intercostal, and gluteus muscle in *Etv1*$^{-/-}$;*mlc1NT3* mice revealed vGluT1^{+} SSEs in all three muscles (Figure 7D, data not shown). Morphologically the "restored" spindles were highly disorganized, however, and often extended much of the length of the intrafusal muscle fiber (Figure 7D). Nevertheless, these results further support a view in which NT3, and its muscle-by-muscle variation in expression level, sets the status of Etv1-dependence for pSNs.

DISCUSSION

The diversification of pSNs into discrete functional subclasses drives the assembly of spinal sensory-motor circuits, but the elemental units of sensory diversity and their molecular origins have remained obscure. We report here that developing pSNs destined to innervate different muscle targets exhibit a marked variability in dependence on the ETS transcription factor Etv1, both for survival and differentiation. The positional basis of Etv1-dependence appears to reflect muscle-by-muscle differences in the level of NT3 expression by embryonic skeletal muscles, and implies the existence of an Etv1-bypass pathway that is progressively recruited by increasing levels of TrkC signaling in proprioceptors. In the absence of known transcriptional determinants of proprioceptor subtype, our findings raise the possibility that certain aspects of pSN diversity are determined by graded variation in the strength of extrinsic signaling rather than by subclass-specific expression of intrinsic transcriptional determinants.

Graded NT3 Signaling and the Grain of Proprioceptor Identity

Our analysis of sensory neuron differentiation has uncovered a previously unappreciated feature of pSN diversity: the mosaic, muscle-by-muscle, dependence on Etv1 for pSN survival. The status of Etv1-sensitivity correlates inversely with muscle NT3 levels: muscles innervated by Etv1-dependent pSNs express ~5-fold lower NT3 levels than muscles innervated by Etv1-independent pSNs. A causal role for NT3 in pSN diversification is suggested by the observation that elevation of muscle NT3 levels in *Etv1*$^{-/-}$ mice restores Etv1-sensitive pSN neuronal number, intraspinal sensory axonal projections, and innervation of muscle spindles. These observations extend earlier studies (Li et al., 2006). They argue that elevated NT3 signaling activates downstream pathways similar or identical to those activated by Etv1 itself, but does so to differing degrees depending on precise muscle target (Figure 8A). We speculate that in addition to promoting pSN survival, graded NT3 signaling may also elicit distinct molecular responses in pSNs innervating different muscle targets, thus contributing to the functional diversity of pSNs. Indeed, changing muscle NT3 expression levels in transgenic mice has been reported to erode the selective connectivity of proprioceptive afferents with target MNs (Wang et al., 2007). Furthermore, recent studies have demonstrated profound changes in gene expression in pSNs in response to elevated NT3 signaling (Lee et al., 2012).

Our findings have not yet resolved whether Etv1 controls pSN survival through direct or indirect actions. The early loss of pSNs in *Etv1* mutants could reflect a direct action of Etv1 in repressing core apoptotic programs that govern pSN survival. Because Etv1 expression in pSNs is induced by NT3 signaling (Patel et al., 2003), it could serve as a transcriptional intermediary in the trophic factor-mediated repression of apoptotic programs (Figure 8B). The idea of an antiapoptotic function for Etv1, restricted to a select neuronal subtype, bears similarities to the role of the Ces-2 transcription factor in *C. elegans*, which engages in dedicated pathways that control apoptosis in neuronal subsets (Metzstein et al., 1996).

NIH-PA Author Manuscript

NIH-PA Author Manuscript

NIH-PA Author Manuscript

Moreover, in spinal neurons, the Ces2-related transcription factor E4PB4 has been shown to act in conjunction with extracellular signaling pathways to regulate the survival of MNs (Junghans et al., 2004). Alternatively, Etv1 could control pSN survival indirectly, through regulation of other ancillary aspects of differentiation that impinge on apoptotic pathways (Figure 8B). A broader role for Etv1 in the regulation of pSN differentiation is suggested by the observation that although pSNs survive in *Etv1*$^{-/-}$;*Bax1*$^{-/-}$ mice, their cell bodies are smaller, and their axons express reduced levels of proprioceptor markers such as Pv and vGluT1 and fail to form normal ventrolateral projections. In addition, pSNs remaining in *Etv1* mutants exhibit abnormal intramuscular sensory terminal morphologies and many fail to induce a normal spindle developmental program (as revealed by lack of *Egr3:WGA* expression in MS intrafusal fibers).

Proprioceptors exhibit a mosaic muscle-by-muscle sensitivity to the loss of Etv1, with pSNs innervating hypaxial and axial muscles most affected, and pSNs innervating certain hindlimb muscles unaffected. This muscle by muscle distinction led us to consider whether there might be a biomechanical logic to the assignment of Etv1-dependent status/NT3 signaling level to individual pSN-muscle units. Within the hindlimb, Etv1-dependence exhibited no obvious correlation with fast or slow muscle fiber type, with extensor and flexor function, or with proximodistal joint control. Nevertheless, it is notable that many limb muscles deprived of sensory innervation in *Etv1* mutants function either as adductors or abductors–notably the gluteus, biceps femoris, and adductor muscles (Figures 4A, 4D, and data not shown). pSNs innervating adductor and abductor muscles have been reported to share one organizational feature with pSNs innervating axial and hypaxial muscles: both sets of sensory neurons lack group Ia reciprocal inhibitory circuitry (Sears, 1964; Jankowska and Odutola, 1980; Eccles and Lundberg, 1958). Thus, one potential role for the pSN NT3-Etv1 signaling cassette could be to confer pSN properties that help in organizing spinal microcircuits so as to fit optimally, the biomechanical demands of their target muscle group.

Transcriptional Control of Proprioceptor Differentiation

Prior studies have shown that at early developmental stages, the activity of Rx3 serves to promote generic pSN identity by repressing expression of TrkB, and maintaining TrkC expression (Kramer et al., 2006; J.C.d.N. and T.M.J., unpublished data; Figure 8B). Our present work indicates that Rx3 may also control aspects of the mature generic pSN phenotype. We find that, in addition to pSNs, Rx3 expression defines a class of mechanoreceptive sensory neurons innervating Merkel cells (Figures 1K and S3), raising the possibility of a functional link between Rx3 expressing pSNs and these cutaneous mechanoreceptors. As with pSNs, Merkel cell afferents depend on NT3 for their survival (Fundin et al., 1997). In addition, these two neuronal sets exhibit similar dynamic properties —pSNs and Merkel cell afferents are the major classes of slowly adapting (SA) mechanoreceptive afferents (Matthews, 1972; Johnson, 2001). Thus, in addition to a generic role in conferring trophic factor sensitivity, Rx3 may regulate the stimulus adaptation kinetics of pSN and SA-cutaneous mechanoreceptors.

Etv1 and Runx3 are expressed by all proprioceptive sensory neurons. So how do these transcription factors also direct pSN subtype character? Within the pSN population, graded Runx3 activity levels may contribute to the specification of MS and GTO pSN subclass character (Figure 8B). Altering the level of Rx3 activity in pSNs systematically changes the dorsoventral termination zone of proprioceptive axon collaterals in the developing chick spinal cord, consistent with the idea that Rx3 activity levels help to specify the distinction between pSNs innervating MSs and GTOs (Chen et al., 2006). The graded activity of Rx3 signaling has recently been suggested to direct the extent of the peripheral growth of pSN axons (Lallemend et al., 2012), providing additional support for the idea that differences in Rx3 activity and/or expression level govern pSN phenotype. A somewhat analogous

NIH-PA Author Manuscript

NIH-PA Author Manuscript

NIH-PA Author Manuscript

function in the regulation of MS pSN phenotype was originally suggested for Etv1, based on the observation that in *Etv1* mutant mice the dorsoventral projection zone of MS pSNs maps to the domain normally occupied by pSNs innervating GTOs (Arber et al., 2000). The pronounced impact of Etv1-inactivation on the survival and morphological differentiation of pSNs innervating both MSs and GTOs, leads us to favor the view that the regional location of muscle target is a more relevant determinant of Etv1-sensitivity than MS or GTO subtype character.

The differential activity of the NT3-Etv1 signaling cassette, as well as that of Rx3, suggests that graded transcription factor activities may be a common theme in the regulation of pSN subclass identity. It is notable that other transcription factors that delineate pSN subclasses have not been identified. Yet, the subtype expression of pSN surface markers, notably members of the Plexin and Cadherin families (Pecho-Vrieseling et al., 2009, Demireva et al., 2011) hints at the existence of distinct transcriptional programs of gene expression in different pSN subtypes. However, many aspects of pSN subclass identity, dorsoventral axonal termination as one example, may rely on incremental rather than discrete phenotypic distinctions, and thus could be achieved through graded Rx3 and NT3-Etv1 signaling.

The fine subtype identity of spinal motor neurons, evident in the organization of MN pools and their dendritic arborization patterns are also regulated through ETS transcription factor signaling, in response to peripheral trophic signals (Haase et al., 2002; Livet et al., 2002), suggesting that ETS transcription factors play a general role as mediators of peripherally induced signals for sensory-motor connectivity. Our studies raise the possibility that extrinsic signals play a prominent role in regulating pSN subtype identity. Linking the transcriptional activities of Rx3 and Etv1 to peripheral NT3 signaling could serve to optimize the fine tuning of diverse pSN subclasses in anticipation of the task of connecting with peripheral muscle and central neuronal targets during development.

EXPERIMENTAL PROCEDURES

Mouse Strains and Animal Husbandry

Mouse strains are described in Table S2. *Runx3:Cre^{ER}* and *Egr3:WGA* animals were generated as described in Supplemental Experimental Procedures. Tamoxifen (Sigma) was administered by a single intraperitoneal (i.p.) injection (5 mg in sesame oil) to pregnant females at e.15.5–e17.5. All animal experiments were performed according to Columbia University guidelines.

In Situ Hybridization Histochemistry and Immunohistochemistry

In situ hybridization histochemistry was performed on cryostat sections using digoxigenin (DIG)-labeled cRNA probes (Arber et al., 2000). Immunohistochemistry was performed on cryostat (15 μm), or vibratome (80–150 μm) sections, or on whole mount preparations (Hantman and Jessell, 2010; Demireva et al., 2011). Primary and secondary antibodies used in experiments are described in Supplemental Experimental Procedures. β-galactosidase analysis was performed as described (Arber et al., 2000). Images were acquired on Zeiss LSM510 confocal microscopes.

Retrograde Labeling of Proprioceptive Afferent Collateral Projections

Dorsal roots of p4–6 pups were dissected-free in ice-cold oxygenated modified artificial cerebrospinal fluid (mACSF) (Hantman and Jessell, 2010) and mounted onto glass capillaries containing 10% rhodamine-dextran (RhD; 3,000 Da MW, Invitrogen) in PBS for 12–14 hr at RT while maintained in oxygenated ACSF solution. Tissue was fixed and processed for vibratome sectioning and confocal analysis.

NIH-PA Author Manuscript

NIH-PA Author Manuscript

NIH-PA Author Manuscript

For CTB labeling, p14–16 animals were anesthetized by Avertin (0.4 g/kg body weight, administered i.p.), and ~0.5 μl of a 1% solution of CTB (List Biologicals) was injected in axial, intercostal, body wall, or hindlimb muscles. After 5 days, animals were processed for analysis.

Neuronal and SSE Counts and Quantification of Cell Size and Collateral Projections

Neuronal cell counts were performed on serial sections (30 μm) of individual DRG, or on cryostat sections obtained from lumbar DRG. We measured the maximal diameter of cell bodies using Zeiss LSM software (Carl Zeiss). Measurements were obtained from cells from cryostat sections. Generally, neuronal counts and cell size measurements were performed on three or more animals/genotype. Counts for sensory endings within muscle spindles were based on the detection of vGluT1 $^{+}$ terminals with characteristic annulospiral morphology. For axial and hypaxial muscle, vGluT1^{+} SSEs were counted in similar regions across all genotypes (see Supplemental Experimental Procedures for details). For limb muscles, vGluT1^{+}sensory terminals (excluding GTO endings) were counted within each individual muscle. Analysis of pSN axonal density was performed using ImageJ analysis software as described in Supplemental Experimental Procedures. Statistical analysis was performed using Student's t test or Mann-Whitney U test.

Quantitative Real-Time PCR

Embryonic muscles were dissected in ice-cold PBS, homogenized in lysis buffer, and total RNA was isolated (RNA isolation kit, Agilent Technologies). qRT-PCR was performed on triplicates using SYBR green on a Stratagene MX3000 thermocycler (Applied Biosystems). Ct values were determined using the automatic baseline determination feature on the Stratagene MX3000 and the relative expression of *NT3* was determined by using the expression $2^{-\Delta Ct}$ (Livak and Schmittgen, 2001). Primer sequences: *NT3* forward 5′-CTGCCACGATCTTACAGGTG-3′, *NT3* reverse 5′-TCCTTTGATC CATGCTGTTG-3′, *MyoD* forward 5′-GGCTACGACACCGCCTACTA-3′, *MyoD* reverse 5′-CACTATGCTGGACAGGCAGT-3′.

Supplementary Material

Refer to Web version on PubMed Central for supplementary material.

Acknowledgments

We thank Andy Liu and Ira Schieren for technical help, Barbara Han, Susan Brenner-Morton, Monica Mendelsohn, and Jennifer Kirkland for help with generation of antibodies and mouse strains, Neil Shneider for providing the *hEGR3* promoter construct and information on its MS expression, and Stèphane Nèdelec and Annina DeLeo for advice on qRT-PCR experiments. We are grateful to S. Arber, D. Wright, W. Snider, and S. Dufour for mouse strains, and to Eiman Azim, Jay Bikoff, Nikolaos Balaskas, George Mentis, Sebastian Poliak, and Niccolo Zampieri for comments on the manuscript. J.C.N. was supported by a Helen Hay Whitney Foundation fellowship. T.M.J. was supported by NIH grant NS033245, the Harold and Leila Y. Mathers Foundation, and Project A.L.S. T.M.J. is an HHMI Investigator.

REFERENCES

Arber S, Ladle DR, Lin JH, Frank E, Jessell TM. ETS gene Er81 controls the formation of functional connections between group Ia sensory afferents and motor neurons. Cell. 2000; 101:485–498. [PubMed: 10850491]

Banks RW, Hulliger M, Saed HH, Stacey MJ. A comparative analysis of the encapsulated end-organs of mammalian skeletal muscles and of their sensory nerve endings. J. Anat. 2009; 214:859–887. [PubMed: 19538631]

NIH-PA Author Manuscript

NIH-PA Author Manuscript

NIH-PA Author Manuscript

Bates B, Rios M, Trumpp A, Chen C, Fan G, Bishop JM, Jaenisch R. Neurotrophin-3 is required for proper cerebellar development. Nat. Neurosci. 1999; 2:115–117. [PubMed: 10195193]

Brown, AG. Organization in the Spinal Cord. New York: Springer; 1981.

Chen AI, de Nooij JC, Jessell TM. Graded activity of transcription factor Runx3 specifies the laminar termination pattern of sensory axons in the developing spinal cord. Neuron. 2006; 49:395–408. [PubMed: 16446143]

Copray JC, Brouwer N. rSelective expression of neurotrophin-3 messenger RNA in muscle spindles of the rat. Neuroscience. 1994; 63:1125–1135. [PubMed: 7700514]

Dasen JS, Jessell TM. Hox networks and the origins of motor neuron diversity. Curr. Top. Dev. Biol. 2009; 88:169–200. [PubMed: 19651305]

Demireva EY, Shapiro LS, Jessell TM, Zampieri N. Motor neuron position and topographic order imposed by β- and γ-catenin activities. Cell. 2011; 147:641–652. [PubMed: 22036570]

Dykes IM, Tempest L, Lee SI, Turner EE. Brn3a and Islet1 act epistatically to regulate the gene expression program of sensory differentiation. J. Neurosci. 2011; 31:9789–9799. [PubMed: 21734270]

Eccles JC, Eccles RM, Lundberg A. The convergence of monosynaptic excitatory afferents on to many different species of alpha motoneurones. J. Physiol. 1957; 137:22–50. [PubMed: 13439582]

Eccles RM, Lundberg A. Integrative pattern of Ia synaptic actions on motoneurones of hip and knee muscles. J. Physiol. 1958; 144:271–298. [PubMed: 13611693]

Fariñas I, Jones KR, Backus C, Wang XY, Reichardt LF. Severe sensory and sympathetic deficits in mice lacking neurotrophin-3. Nature. 1994; 369:658–661. [PubMed: 8208292]

Fariñas I, Yoshida CK, Backus C, Reichardt LF. Lack of neurotrophin-3 results in death of spinal sensory neurons and premature differentiation of their precursors. Neuron. 1996; 17:1065–1078. [PubMed: 8982156]

Fundin BT, Silos-Santiago I, Ernfors P, Fagan AM, Aldskogius H, DeChiara TM, Phillips HS, Barbacid M, Yancopoulos GD, Rice FL. Differential dependency of cutaneous mechanoreceptors on neurotrophins, trk receptors, and P75 LNGFR. Dev. Biol. 1997; 190:94–116. [PubMed: 9331334]

Gong S, Zheng C, Doughty ML, Losos K, Didkovsky N, Schambra UB, Nowak NJ, Joyner A, Leblanc G, Hatten ME, Heintz N. A gene expression atlas of the central nervous system based on bacterial artificial chromosomes. Nature. 2003; 425:917–925. [PubMed: 14586460]

Haase G, Dessaud E, Garcè s A, de Bovis B, Birling M, Filippi P, Schmalbruch H, Arber S, deLapeyrière O. GDNF acts through PEA3 to regulate cell body positioning and muscle innervation of specific motor neuron pools. Neuron. 2002; 35:893–905. [PubMed: 12372284]

Hantman AW, Jessell TM. Clarke's column neurons as the focus of a corticospinal corollary circuit. Nat. Neurosci. 2010; 13:1233–1239. [PubMed: 20835249]

Hinterberger TJ, Sassoon DA, Rhodes SJ, Konieczny SF. Expression of the muscle regulatory factor MRF4 during somite and skeletal myofiber development. Dev. Biol. 1991; 147:144–156. [PubMed: 1715299]

Hippenmeyer S, Shneider NA, Birchmeier C, Burden SJ, Jessell TM, Arber S. A role for neuregulin1 signaling in muscle spindle differentiation. Neuron. 2002; 36:1035–1049. [PubMed: 12495620]

Hippenmeyer S, Vrieseling E, Sigrist M, Portmann T, Laengle C, Ladle DR, Arber S. A developmental switch in the response of DRG neurons to ETS transcription factor signaling. PLoS Biol. 2005; 3:e159. [PubMed: 15836427]

Iscoe S. Segmental responses of abdominal motoneurons in decerebrate cats. Respir. Physiol. 2000; 122:27–34. [PubMed: 10936598]

Jankowska E, Odutola A. Crosses and uncrossed synaptic actions on motoneurones of back muscles in the cat. Brain Res. 1980; 194:65–78. [PubMed: 6445769]

Jessell TM, Sürmeli G, Kelly JS. Motor neurons and the sense of place. Neuron. 2011; 72:419–424. [PubMed: 22078502]

Johnson KO. The roles and functions of cutaneous mechanoreceptors. Curr. Opin. Neurobiol. 2001; 11:455–461. [PubMed: 11502392]

NIH-PA Author Manuscript

NIH-PA Author Manuscript

NIH-PA Author Manuscript

Junghans D, Chauvet S, Buhler E, Dudley K, Sykes T, Henderson CE. The CES-2-related transcription factor E4BP4 is an intrinsic regulator of motoneuron growth and survival. Development. 2004; 131:4425–4434. [PubMed: 15306565]

Kanning KC, Kaplan A, Henderson CE. Motor neuron diversity in development and disease. Annu. Rev. Neurosci. 2010; 33:409–440. [PubMed: 20367447]

Klein R, Silos-Santiago I, Smeyne RJ, Lira SA, Brambilla R, Bryant S, Zhang L, Snider WD, Barbacid M. Disruption of the neurotrophin-3 receptor gene trkC eliminates la muscle afferents and results in abnormal movements. Nature. 1994; 368:249–251. [PubMed: 8145824]

Kramer I, Sigrist M, de Nooij JC, Taniuchi I, Jessell TM, Arber S. A role for Runx transcription factor signaling in dorsal root ganglion sensory neuron diversification. Neuron. 2006; 49:379–393. [PubMed: 16446142]

Lallemend F, Ernfors P. Molecular interactions underlying the specification of sensory neurons. Trends Neurosci. 2012; 35:373–381. [PubMed: 22516617]

Lallemend F, Sterzenbach U, Hadjab-Lallemend S, Aquino JB, Castelo-Branco G, Sinha I, Villaescusa JC, Levanon D, Wang Y, Franck MC, et al. Positional differences of axon growth rates between sensory neurons encoded by Runx3. EMBO J. 2012; 31:3718–3729. [PubMed: 22903063]

Landmesser L. The distribution of motoneurones supplying chick hind limb muscles. J. Physiol. 1978; 284:371–389. [PubMed: 731549]

Lee J, Friese A, Mielich M, Sigrist M, Arber S. Scaling proprioceptor gene transcription by retrograde NT3 signaling. PLoS ONE. 2012; 7:e45551. [PubMed: 23029089]

Levine AJ, Lewallen KA, Pfaff SL. Spatial organization of cortical and spinal neurons controlling motor behavior. Curr. Opin. Neurobiol. 2012; 22:812–821. [PubMed: 22841417]

Li LY, Wang Z, Sedý J, Quazi R, Walro JM, Frank E, Kucera J. Neurotrophin-3 ameliorates sensory-motor deficits in Er81-deficient mice. Dev. Dyn. 2006; 235:3039–3050. [PubMed: 17013886]

Livak KJ, Schmittgen TD. Analysis of relative gene expression data using real-time quantitative PCR and the 2(-Delta Delta C(T)) method. Methods. 2001; 25:402–408. [PubMed: 11846609]

Livet J, Sigrist M, Stroebel S, De Paola V, Price SR, Henderson CE, Jessell TM, Arber S. ETS gene Pea3 controls the central position and terminal arborization of specific motor neuron pools. Neuron. 2002; 35:877–892. [PubMed: 12372283]

Ma Q, Fode C, Guillemot F, Anderson DJ. Neurogenin1 and neurogenin2 control two distinct waves of neurogenesis in developing dorsal root ganglia. Genes Dev. 1999; 13:1717–1728. [PubMed: 10398684]

Madisen L, Zwingman TA, Sunkin SM, Oh SW, Zariwala HA, Gu H, Ng LL, Palmiter RD, Hawrylycz MJ, Jones AR, et al. A robust and high-throughput Cre reporting and characterization system for the whole mouse brain. Nat. Neurosci. 2010; 13:133–140. [PubMed: 20023653]

Matthews, PBC. Mammalian Muscle Receptors and Their Central Actions. London: Edward Arnold Publishers; 1972.

Mears SC, Frank E. Formation of specific monosynaptic connections between muscle spindle afferents and motoneurons in the mouse. J. Neurosci. 1997; 17:3128–3135. [PubMed: 9096147]

Mendelson B, Frank E. Specific monosynaptic sensory-motor connections form in the absence of patterned neural activity and motoneuronal cell death. J. Neurosci. 1991; 11:1390–1403. [PubMed: 2027053]

Metzstein MM, Hengartner MO, Tsung N, Ellis RE, Horvitz HR. Transcriptional regulator of programmed cell death encoded by Caenorhabditis elegans gene ces-2. Nature. 1996; 382:545–547. [PubMed: 8700229]

Molander C, Grant G. Laminar distribution and somatotopic organization of primary afferent fibers from hindlimb nerves in the dorsal horn. A study by transganglionic transport of horseradish peroxidase in the rat. Neuroscience. 1986; 19:297–312. [PubMed: 3785668]

Nakayama K, Niwa M, Sasaki SI, Ichikawa T, Hirai N. Morphology of single primary spindle afferents of the intercostal muscles in the cat. J. Comp. Neurol. 1998; 398:459–472. [PubMed: 9717703]

Patel TD, Kramer I, Kucera J, Niederkofler V, Jessell TM, Arber S, Snider WD. Peripheral NT3 signaling is required for ETS protein expression and central patterning of proprioceptive sensory afferents. Neuron. 2003; 38:403–416. [PubMed: 12741988]

NIH-PA Author Manuscript

NIH-PA Author Manuscript

NIH-PA Author Manuscript

Pecho-Vrieseling E, Sigrist M, Yoshida Y, Jessell TM, Arber S. Specificity of sensory-motor connections encoded by Sema3e-Plxnd1 recognition. Nature. 2009; 459:842–846. [PubMed: 19421194]

Pierrot-Deseilligny, E.; Burke, D. The Circuitry of the Human Spinal Cord. Cambridge: Cambridge University Press; 2005.

Pietri T, Eder O, Blanche M, Thiery JP, Dufour S. The human tissue plasminogen activator-Cre mouse: a new tool for targeting specifically neural crest cells and their derivatives in vivo. Dev. Biol. 2003; 259:176–187. [PubMed: 12812797]

Romanes GJ. The motor cell columns of the lumbo-sacral spinal cord of the cat. J. Comp. Neurol. 1951; 94:313–363. [PubMed: 14832391]

Sears TA. Some properties and reflex connexions of respiratory motoneurones of the cat's thoracic spinal cord. J. Physiol. 1964; 175:386–403. [PubMed: 14241839]

Taylor MD, Vancura R, Patterson CL, Williams JM, Riekhof JT, Wright DE. Postnatal regulation of limb proprioception by muscle-derived neurotrophin-3. J. Comp. Neurol. 2001; 432:244–258. [PubMed: 11241389]

Tourtellotte WG, Milbrandt J. Sensory ataxia and muscle spindle agenesis in mice lacking the transcription factor Egr3. Nat. Genet. 1998; 20:87–91. [PubMed: 9731539]

Vanderhorst VG, Holstege G. Organization of lumbosacral motoneuronal cell groups innervating hindlimb, pelvic floor, and axial muscles in the cat. J. Comp. Neurol. 1997; 382:46–76. [PubMed: 9136811]

Wang Z, Li LY, Taylor MD, Wright DE, Frank E. Prenatal exposure to elevated NT3 disrupts synaptic selectivity in the spinal cord. J. Neurosci. 2007; 27:3686–3694. [PubMed: 17409232]

White FA, Keller-Peck CR, Knudson CM, Korsmeyer SJ, Snider WD. Widespread elimination of naturally occurring neuronal death in Bax-deficient mice. J. Neurosci. 1998; 18:1428–1439. [PubMed: 9454852]

Windhorst U. Muscle proprioceptive feedback and spinal networks. Brain Res. Bull. 2007; 73:155–202. [PubMed: 17562384]

Wu SX, Koshimizu Y, Feng YP, Okamoto K, Fujiyama F, Hioki H, Li YQ, Kaneko T, Mizuno N. Vesicular glutamate transporter immunoreactivity in the central and peripheral endings of muscle-spindle afferents. Brain Res. 2004; 1011:247–251. [PubMed: 15157812]

Xiang M, Gan L, Li D, Zhou L, Chen ZY, Wagner D, O'Malley BW Jr. Klein W, Nathans J. Role of the Brn-3 family of POU-domain genes in the development of the auditory/vestibular, somatosensory, and visual systems. Cold Spring Harb. Symp. Quant. Biol. 1997; 62:325–336. [PubMed: 9598366]

Yoshihara Y. Visualizing selective neural pathways with WGA trans-gene: combination of neuroanatomy with gene technology. Neurosci. Res. 2002; 44:133–140. [PubMed: 12354628]

Zhao J, Nassar MA, Gavazzi I, Wood JN. Tamoxifen-inducible NaV1.8-CreERT2 recombinase activity in nociceptive neurons of dorsal root ganglia. Genesis. 2006; 44:364–371. [PubMed: 16850455]

NIH-PA Author Manuscript
NIH-PA Author Manuscript
NIH-PA Author Manuscript

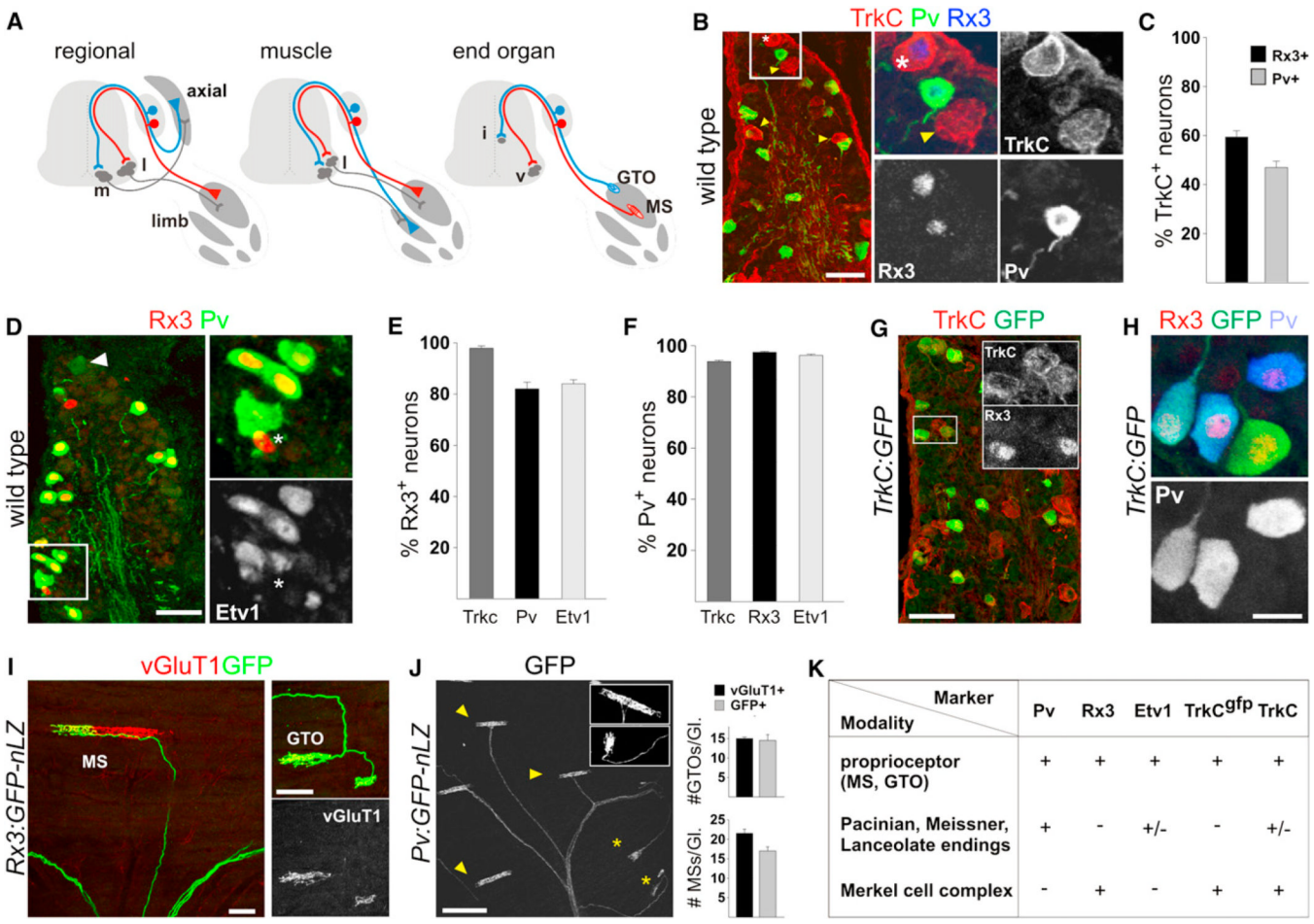

K

Modality \ Marker	Pv	Rx3	Etv1	TrkC^{gfp}	TrkC
proprioceptor (MS, GTO)	+	+	+	+	+
Pacinian, Meissner, Lanceolate endings	+	-	+/-	-	+/-
Merkel cell complex	-	+	-	+	+

Figure 1. Proprioceptive Sensory Neurons Express TrkC, Rx3, Pv, and Etv1

(A) Schematic illustration of proprioceptor subtype identities. According to subtype identity, proprioceptors exhibit distinct intraspinal collateral trajectories, terminating in medial (m), lateral (l), intermediate (i), or ventral (v) spinal cord.

(B) Expression of TrkC, Rx3, and Pv in wild-type rostral lumbar DRG at p0. Arrowheads indicate TrkC^{+}Rx3^{off}Pv^{off}neurons. Asterisk shows a TrkC^{+}Rx3^{+}Pv^{off} neuron. Enlarged (boxed) area shows marker expression individually.

(C) Percentage of TrkC^{+} sensory neurons expressing Rx3 or Pv in rostral lumbar DRG at p0.

(D) Expression of Pv, Rx3 and Etv1 in wild-type rostral lumbar DRG at p0. Arrow head indicates a Pv^{+}Rx3^{off}Etv1^{off} neuron. Boxed area is enlarged to indicate Rx3^{+}Pv^{off}Etv1 ^{off}neurons (asterisk).

(E) Percentage of Rx3^{+} sensory neurons expressing TrkC, Pv, or Etv1 in rostral lumbar DRG at p0.

(F) Percentage of Pv^{+} sensory neurons expressing TrkC, Rx3, or Etv1 in rostral lumbar DRG at p0.

(G) Expression of TrkC and GFP in *TrkC:GFP* reporter mice in rostral lumbar DRG at p0. Inset (boxed area) shows that expression of GFP is restricted to TrkC^{+}Rx3^{+} neurons.

(H) Expression of Pv in Rx3^{+}GFP^{+} neurons in *TrkC:GFP* reporter mice in rostral DRG at p0.

(I) Peripheral endings in *Rx3:Cre^{ER}/Tau:lsl:mGFP-nLZ (Rx3:mGFP-nLZ)* mice following a single tamoxifen injection at e17.5. Expression of mGFP is observed in a mosaic pattern in vGluT1^{+} MS and GTO endings in p5 gluteus muscle.

NIH-PA Author Manuscript

NIH-PA Author Manuscript

NIH-PA Author Manuscript

(J) $mGFP^+$ MS (arrowheads) and GTO (asterisks) sensory endings in p5 gluteus muscle in *Pv:Cre/Tau:lsl:mGFP-nLZ (Pv:mGFP-nLZ)* mice. Numbers of $mGFP^+$ MSs and GTOs in gluteus muscle of *Pv:mGFP-nLZ* mice are similar to the numbers of $vGluT1^+$ MSs and GTOs in WT gluteus.

(K) Summary of Pv, Rx3, Etv1, TrkC:GFP, and TrkC expression profiles in proprioceptive and cutaneous mechanoreceptive afferents in DRG. (+) denotes “expression,” (−) denotes “no expression,” (+/−) denotes “expression in a subset of neurons.”

Error bars represent SEM. Scale bars represent 20 μm(H), 50 μm (B, D, G, and I), and 200 μm (J). See also Figures S1, S2, S3, and Table S1.

NIH-PA Author Manuscript
NIH-PA Author Manuscript
NIH-PA Author Manuscript

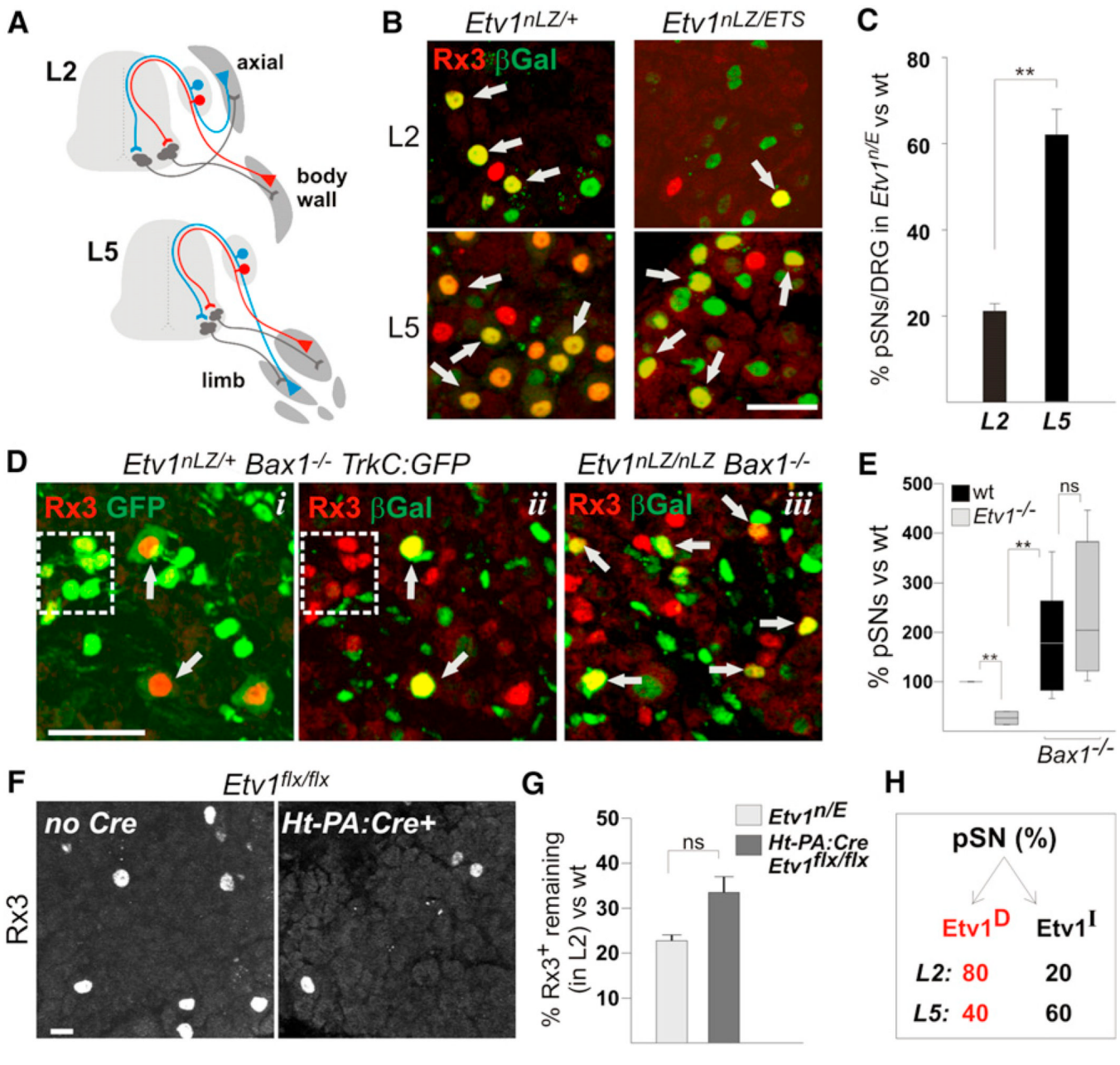

Figure 2. pSN Viability Depends on Etv1

(A) Diagram illustrating the regional identities of rostral lumbar (L1–L2; axial and hypaxial) and caudal lumbar (L3–L5; limb) pSNs.

(B) Expression of Rx3 and Etv1 in L2 and L5 DRG of p0 wild-type (*Etv1*$^{nLZ/+}$) and *Etv1*$^{-/-}$ mice. Arrows indicate pSNs coexpressing Rx3 and Etv1. Expression of Etv1 is visualized using a nuclear β-galactosidase reporter expressed from the *Etv1* locus.

(C) Percentage of pSNs (Rx3^{+}βGal^{+}) in p0 *Etv1*$^{-/-}$ DRG in comparison to wild-type. Average number for wild-type L2: 234.5 pSNs (n = 8 DRG), average number for wild-type L5: 564 pSNs (n = 6). The number of neurons in both *Etv1*$^{-/-}$ L2 (n = 4) and L5 (n = 4) is significantly reduced compared to wild-type (L2 $p < 0.001$; L5 $p < 0.001$; Student's t test), but the loss of pSNs is more severe in L2 than in L5 DRG ($p < 0.001$; Student's t test).

NIH-PA Author Manuscript

NIH-PA Author Manuscript

NIH-PA Author Manuscript

(D) Expression of Rx3, TrkC:GFP, and Etv1 in p1–3 rostral lumbar(L1–L2) DRG of *Bax1*$^{-/-}$ (i and ii) and *Etv1*$^{-/-}$;*Bax1*$^{-/-}$ (iii) mice. Images in (i and ii) are taken of the identical region of the section. Arrows indicate coexpression of Rx3 and TrkC:GFP (i) or Rx3 and βGal (ii and iii). Boxed area in (i and ii) illustrates the small-sized Rx3^{+}GFP^{+} neurons that lack Etv1 in *Bax1*$^{-/-}$ and *Etv1*$^{-/-}$;*Bax1*$^{-/-}$ DRG.

(E) Number of pSNs (Rx3^{+}nLZ^{+})/section in p1–3 rostral lumbar (L1-L2) DRG of *Etv1*$^{-/-}$, *Bax1*$^{-/-}$, and *Etv1*$^{-/-}$;*Bax1*$^{-/-}$ mice compared to wild-type (100% = 7.58 pSNs/section; 19 sections). The percentage of pSNs/section in *Etv1*$^{-/-}$ is significantly different compared to both wild-type and *Etv1*$^{-/-}$;*Bax1*$^{-/-}$ mice ($p < 0.001$), whereas the percentage of pSN/section in *Bax1*$^{-/-}$ and *Etv1*$^{-/-}$;*Bax1*$^{-/-}$ is equivalent ($p = 0.15$; Mann-Whitney U test).

(F) Expression of Rx3 in p6 L2 DRG in wild-type (*Etv1*$^{flx/flx}$ *or Etv1*$^{flx/+}$) and *Ht-PA:Cre;Etv1*$^{flx/flx}$ animals.

(G) Rx3^{+} neurons in L2 DRG in constitutive (*Etv1*$^{-/-}$, n = 3) and sensory neuron-specific *(Ht-PA:Cre;Etv1*$^{flx/flx}$, n = 6) *Etv* 1 mutants ($p = 0.077$, Student's t test).

(H) Schematic illustrates proprioceptor segregation into Etv1-dependent (Etv1^{D}) and Etv1-independent (Etv1^{I}) subsets.

Error bars represent SEM (C, G), or maximum and minimum values (E). Scale bars represent 20 μm (F), 25 μm (D), and 50 μm (B). See also Figure S4 and Table S1.

NIH-PA Author Manuscript

NIH-PA Author Manuscript

NIH-PA Author Manuscript

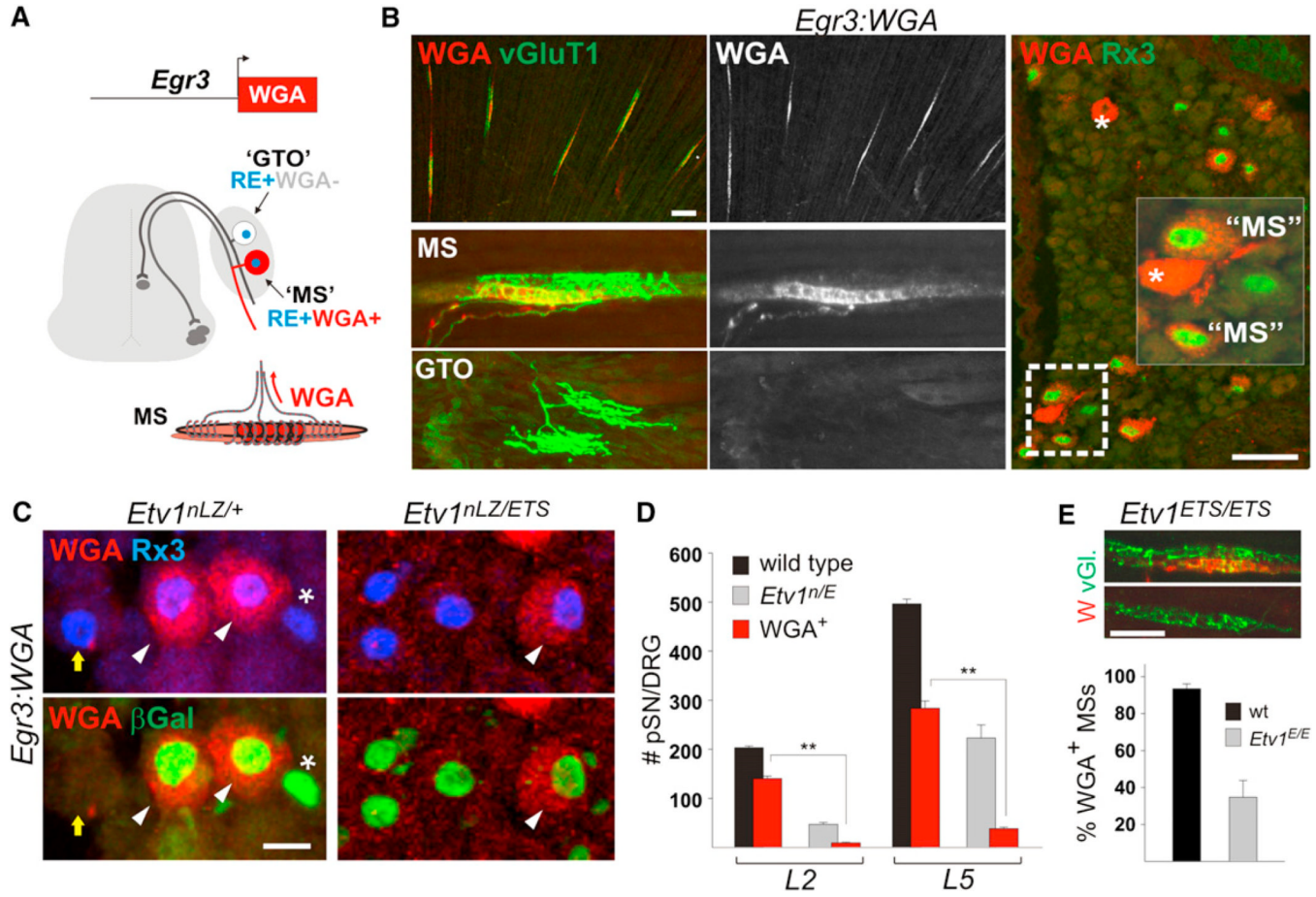

Figure 3. Etv1-Dependence Does Not Segregate with MS pSNs

(A) Genetic strategy to label MS-innervating pSNs in *Egr3:WGA* transgenic mice. WGA expressed in the intrafusal muscle fibers of the muscle spindle is taken up by spindle pSN sensory endings and transported to their ($Rx3^{+}Etv1^{+}$) cell bodies in DRG.

(B) Expression of WGA in p5 gluteus muscle and p7 rostral lumbar DRG in *Egr3:WGA* transgenic mice. Expression of WGA is readily observed in $vGluT1^{+}$ MS sensory endings, but not in GTO endings. In DRG, accumulation of WGA in $Rx3^{+}$ neurons implies they correspond to MS afferents. WGA is also observed in some $Rx3^{off}$ neurons (asterisk), reflecting expression of the human *Egr3* promoter element in a subset of nonproprioceptive peripheral sensory endings.

(C) Expression of Rx3, Etv1 (βGal) and WGA in p7 L2 DRG of $Etv1^{nLZ/+}$*;Egr3:WGA* (WT) and $Etv1^{-/-}$*;EGR3:WGA* mice (images with Rx3/WGA expression are from identical area as images with Etv1 (βGal)/WGA expression). In wild-type, coexpression of Rx3, Etv1, and the accumulation of WGA defines MS-afferent cell bodies (arrow heads). Asterisk indicates a $WGAo^{ff}Rx3^{+}Etv1^{+}$ pSN presumed to correspond to a GTO-afferent. $Rx3^{+}Etv1^{off}$cutaneous mechanoreceptors (arrow) also lack accumulation of WGA. In DRG of $Etv1^{-/-}$ mice, WGA^{+} as well as WGA^{off} pSNs can be observed.

(D) Number of WGA^{+} pSNs (defined by Rx3 and $Etv1^{nLZ}$ coexpression; red bars) in comparison to total numbers of pSNs in wild-type (black bars) and $Etv1^{-/-}$(gray bars) L2 at p7–10(n = 6 DRG for wild-type L2 and L5 *DRG; for* $Etv1^{-/-}$ DRG, n = 6 for L2 and n = 4 for L5).The number of WGA^{+} pSNs in L2 and L5 DRG of *Etv1* mutants is significantly reduced compared to wild-type (L2 $p < 0.001$, L5 $p < 0.001$; Student's t test).

NIH-PA Author Manuscript

NIH-PA Author Manuscript

NIH-PA Author Manuscript

(E) Analysis of WGA expression in MS intrafusal fibers in p5 *Etv1*$^{-/-}$*;EGR3:WGA* Soleus muscle. The number of vGluT1^{+} MS sensory endings that colocalizes with WGA expression is reduced in *Etv1* mutant muscle (sample includes: soleus, medial gastrocnemius, extensor digitorum longus, tibialis anterior, plantaris) when compared to wild-type muscle.
Error bars represent SEM. Scale bars represent 20 μm (C), 50 μm (B; DRG, E) and 100 μm (B; muscle). See also Figure S5 and Table S3.

NIH-PA Author Manuscript
NIH-PA Author Manuscript
NIH-PA Author Manuscript

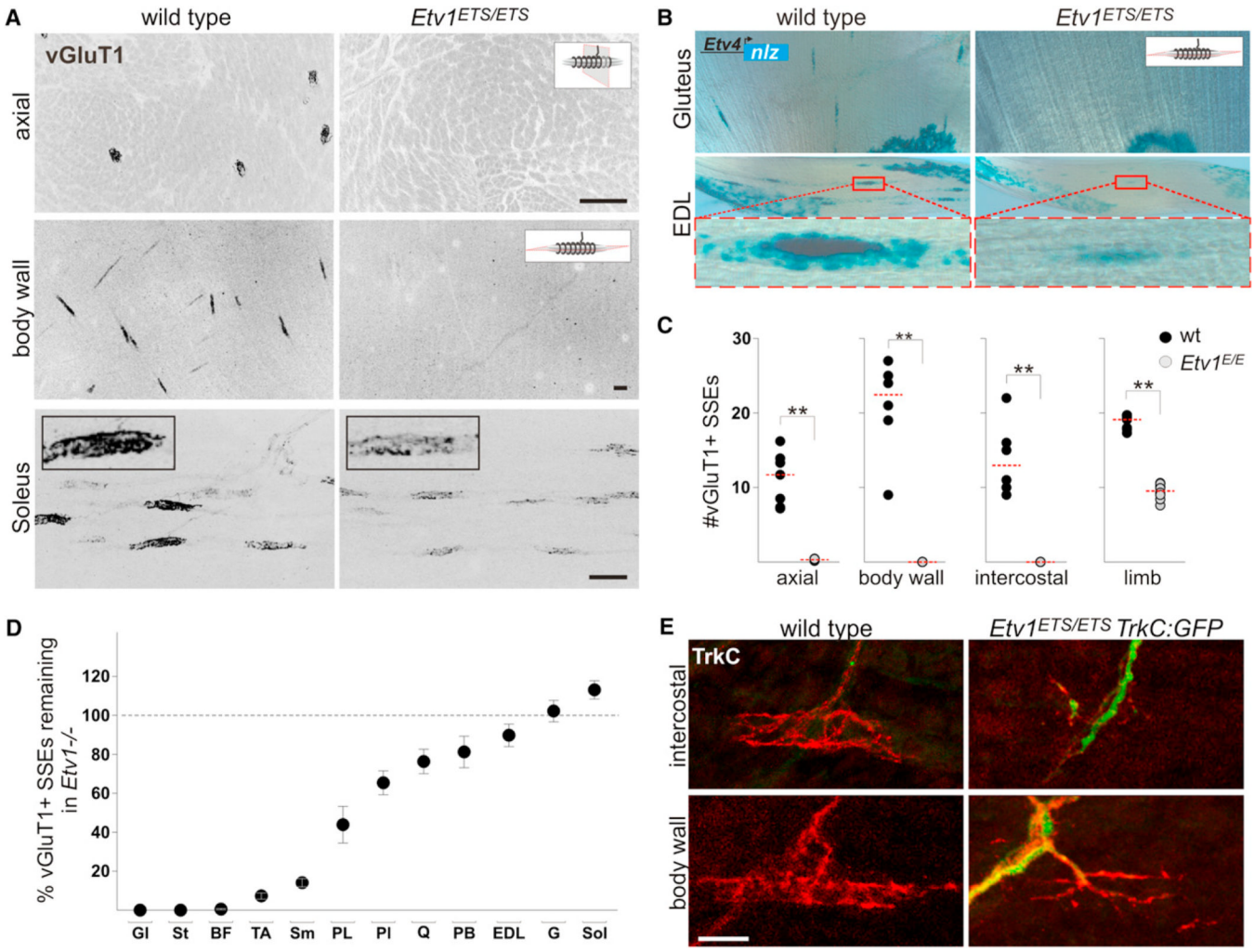

Figure 4. Selective Loss of pSN Innervation in *Etv1* Mutant Mice

(A) Analysis of vGluT1$^+$ spindle-associated sensory endings (SSEs) in axial, hypaxial (body wall), and limb muscle (soleus), in wild-type and *Etv1*$^{-/-}$ mice at p3–5. Insets in soleus panels compare the levels of vGluT1 expression in wild-type and *Etv1*$^{-/-}$ SSEs. Schematic insets indicate plane of image.

(B) Analysis of MSs in hindlimb muscle from wild-type and *Etv1*$^{-/-}$ mice using an *Etv4*^{nLZ} reporter allele expressing βGal in the nuclei of intrafusal muscle fibers. Boxed area shows reduced levels of βGal activity in *Etv1*$^{-/-}$ EDL MS, implying a reduced level of *Etv4* expression.

(C) Number of vGluT1$^+$ SSEs in axial, hypaxial, and limb muscle targets in wild-type and *Etv1*$^{-/-}$*mice*. Individual points represent individual SSE counts in defined area/animal (see Supplemental Experimental Procedures). Counts for limb muscles are the average number of SSEs observed for a set of muscles (described in D)/animal. Median values are represented by a red dotted line. The number of SSEs in *Etv1*$^{-/-}$ muscle was significantly reduced compared to wild-type (Mann-Whitney U test).

(D) Percentage of remaining vGluT1$^+$ SSEs in *Etv1*$^{-/-}$ mice when compared to wild-type. Muscles analyzed were gluteus (Gl), biceps femoris (BF), quadriceps (Q; rectus femoris, vasti), semitendinosus (St), semimembranosus (Sm), gastrocnemius (G; lateral and medial), soleus (Sol), plantaris (Pl), tibialis anterior (TA), extensor digitorum longus (EDL), and peroneus longus (PL) and brevis (PB). Error bars represent SEM. Many muscles showed a

NIH-PA Author Manuscript

NIH-PA Author Manuscript

NIH-PA Author Manuscript

significant reduction in the number of SSEs when compared to wild-type, but others did not (Mann-Whitney U test).

(E) Initial formation of SSEs at e15.5 in hypaxial muscles of wild-type and *Etv1*$^{-/-}$ mice as analyzed by expression of endogenous TrkC protein (wild-type and *Etv1*$^{-/-}$) and the *TrkC:GFP* reporter (*Etv1*$^{-/-}$).

Scale bars represent 20 μm (E) and 100 μm (A). See also Figures S6 and S7.

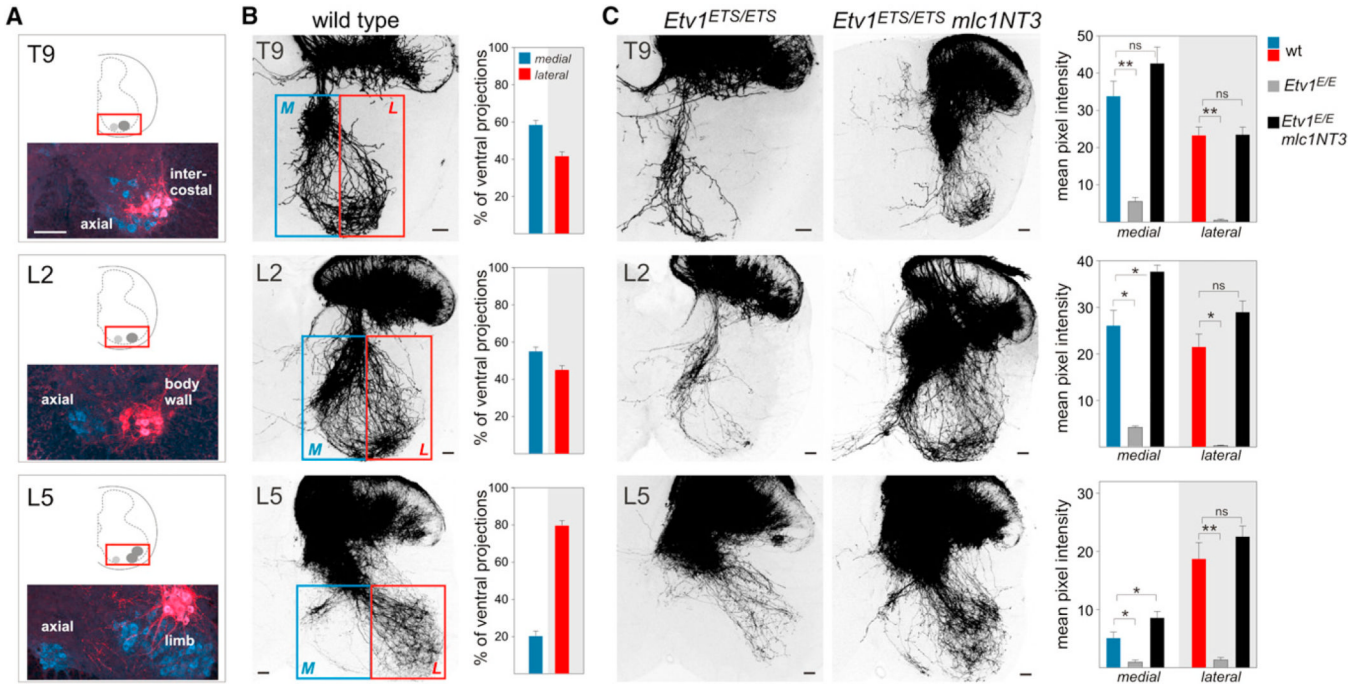

Figure 5. Differential pSN Etv1-Dependence Is Reflected in Central Projection Phenotypes

(A) Choleratoxin-B (CTB) labeling of ($ChaT^+$) motor neurons innervating intercostal, body wall, and distal hindlimb muscle, which are targeted by collaterals from pSNs located in T9, L2, and L5 DRG, respectively.

(B) Collateral trajectories of pSNs residing in T9, L2 and L5 DRG in wild-type at p5–6, visualized using RhD dorsal root fills. Boxed areas indicate the medial (M) and lateral (L) ventral horn compartments used in quantitative analysis comparing the percentage of medial and lateral projections.

(C) Analysis of collateral density of RhD^+ T9, L2, and L5 medial and lateral trajectories in *Etv1*$^{-/-}$and *Etv1*$^{-/-}$*;mlc1NT3*$^+$ mice at p5–6, in comparison to wild-type. Collateral densities were expressed as mean pixel intensity (mpi), calculated using ImageJ analysis software; see Experimental Procedures). Values for M and L cannot be compared across levels as regions are defined differently for each segmental level (see B).

Error bars represent SEM. Scale bars represent 50 μm.

NIH-PA Author Manuscript
NIH-PA Author Manuscript
NIH-PA Author Manuscript

NIH-PA Author Manuscript
NIH-PA Author Manuscript
NIH-PA Author Manuscript

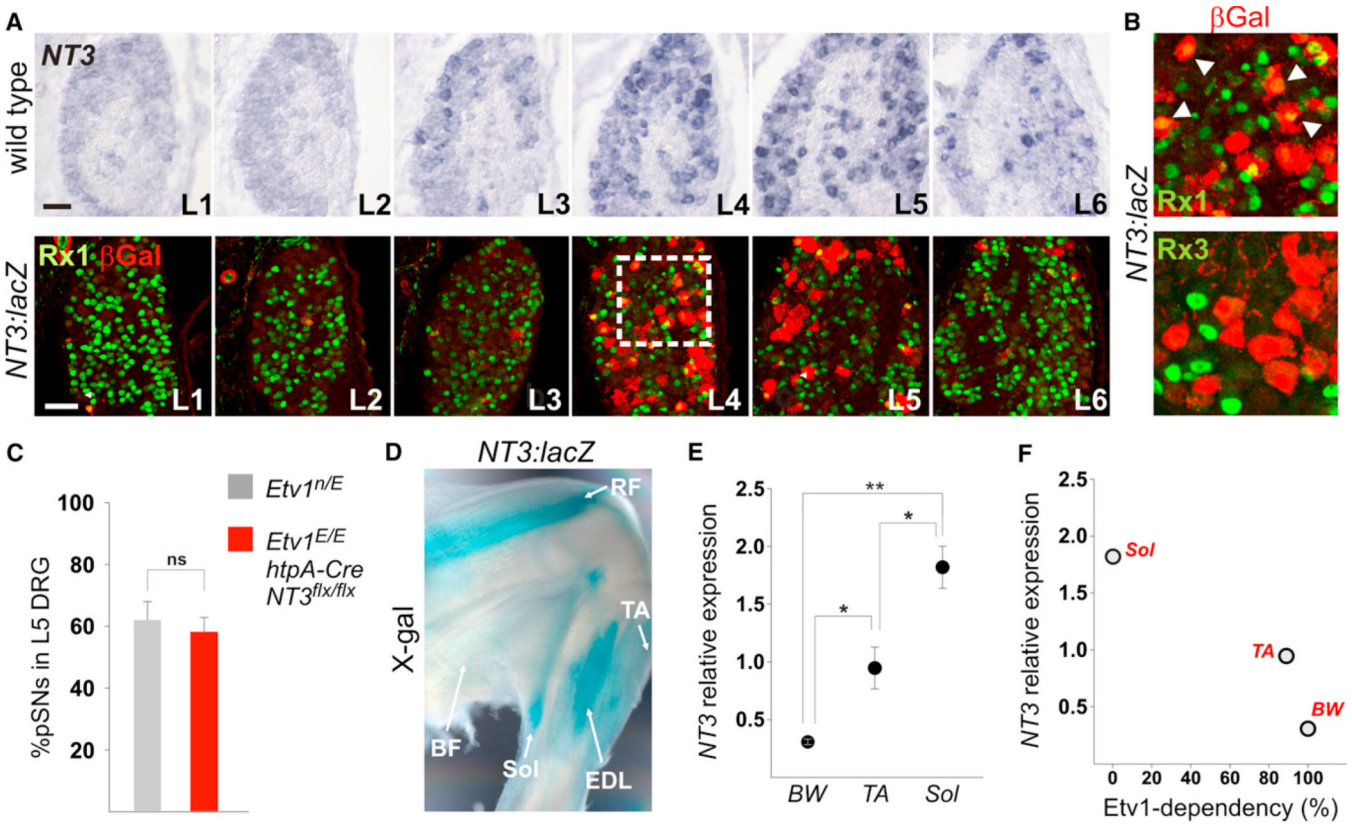

Figure 6. pSN Etv1-Dependence Correlates with Muscle Target NT3 Levels

(A) Expression of *NT3*, βGal (expressed from the *NT3:lacZ* allele), and Rx1 in lumbar DRG at p0. *NT3* and βGal are virtually absent from L1–2 DRG, but are abundantly expressed in L4–L5 DRG. Boxed area is enlarged in (B).

(B) Expression of βGal in L4/5 DRG of *NT3:lacZ* mice can be observed in $Rx1^+$ cutaneous neurons but is excluded from $Rx3^+$ pSNs.

(C) Percentage of pSNs ($Rx3^+Pv^+$) that remains in L5 DRG of $Etv1^{-/-}$(n = 4), and $Etv1^{-/-}$;*Ht-PA:Cre;* $NT3^{flx/flx}$ mice at p0–5 is similar (p = 0.707; Student's t test).

(D) βGal-activity levels in e15.5 embryonic hindlimb muscles of *NT3:lacZ* mice. Muscles indicated are rectus femoris (RF), soleus (Sol), extensor digitorum longus (EDL), Tibialis anterior (TB), and biceps femoris (BF).

(E) Relative quantity of *NT3* mRNA detected by qRT-PCR in embryonic (e15–e16) body wall (BW), tibialis anterior (TA), and soleus (Sol) muscle. Data was obtained from four independent experiments and represent relative quantity normalized to MyoD.

(F) Muscle NT3 expression levels correlate inversely with pSN Etv1-dependence.

Error bars represent SEM. Scale bars represent 50 μm (A).

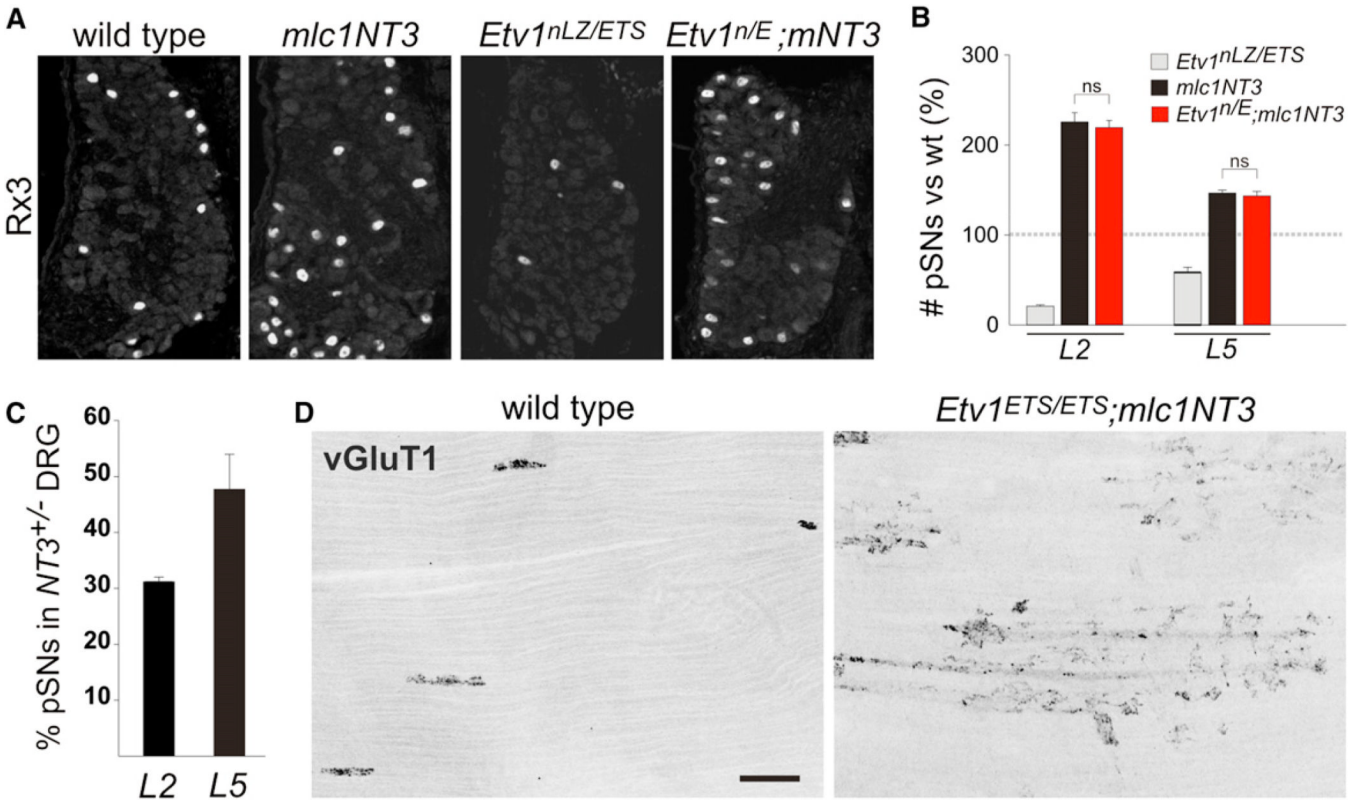

Figure 7. Elevated Levels of Muscle NT3 Ameliorates *Etv1* Mutant Phenotypes

(A) Expression of Rx3 in wild-type, *mlc1NT3*$^{+}$, *Etv1*$^{-/-}$, and *Etv1*$^{-/-}$;*mlc1NT3*$^{+}$ rostral lumbar (L1-L2) DRG at p0.

(B) Percent change in the number of pSNs in L2 and L5 DRG in *Etv1*$^{-/-}$ (L2: n = 4; L5: n = 4), *mlc1NT3*$^{+}$ (L2: n = 6; L5: n = 2) and *Etv1*$^{-/-}$;*mlc1NT3*$^{+}$ (L2: n = 4; L5: n = 4 DRG) mice in comparison to wild-type L2 (n = 8) and L5 (n = 6) DRG at p2–8. The increase in pSNs was not different between *mlc1NT3*$^{+}$ and *Etv1*$^{-/-}$;*mlc1NT3*$^{+}$ DRG (Student's t test). Error bars represent SEM.

(C) Percentage of pSNs in L2 and L5 *NT3*$^{+/-}$ DRG at p0–2 compared to WT.

(D) vGluT1^{+} SSEs in body wall muscle in wild-type and *Etv1*$^{ETS/ETS}$;*mlc1NT3* mice at p7. Scale bar represents 200 μm.

See also Table S2.

NIH-PA Author Manuscript
NIH-PA Author Manuscript
NIH-PA Author Manuscript

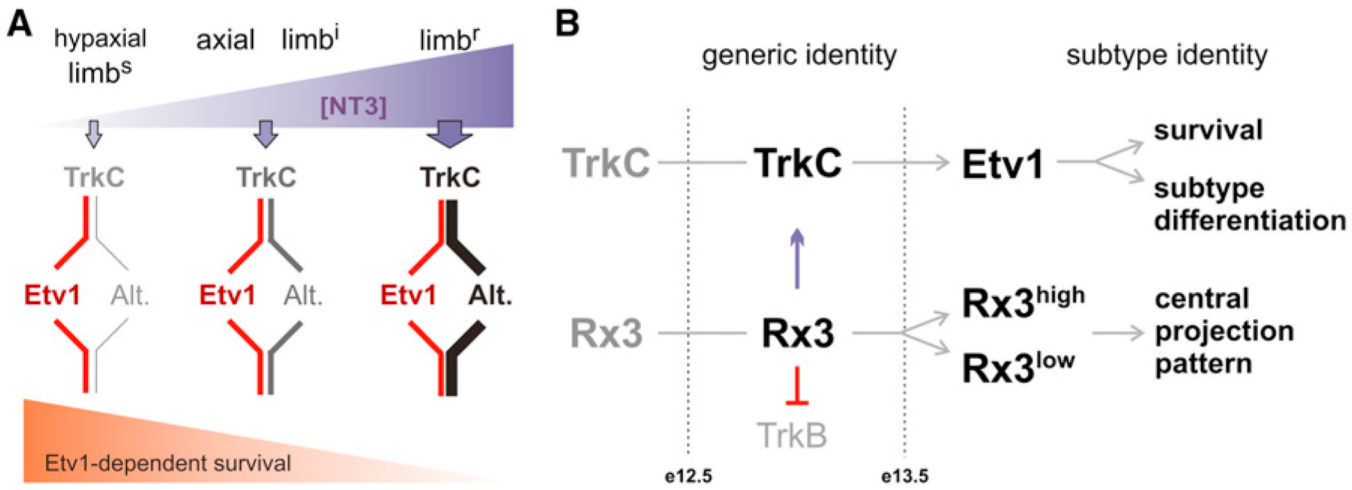

Figure 8. Activities of NT3, Etv1, and Rx3 in pSN Differentiation

(A) Loss of Etv1 uncovers the existence of an alternate (Alt.) NT3-activated signaling pathway that is progressively activated with increased NT3/TrkC signaling. The relative weight of both pathways is a function of the ambient levels of muscle-derived NT3. Both Etv1 and Alt. pathways may control pSN survival and/or subtype specialization, with afferents from hypaxial, axial and certain limb muscles ($limb^s$) primarily dependent on Etv1 signaling, whereas afferents from other limb muscles show an intermediate requirement ($limb^i$) for Etv1 or are refractory ($limb^r$) to the loss of Etv1.

(B) Intersection of TrkC, Rx3, and Etv1 signaling pathways in pSN differentiation. At early stages (e12.5) Rx3 solidifies pSN identity by repressing TrkB and promoting TrkC expression, whereas later (>e13.5) Rx3 activity levels control the extent of pSN collateral projections into the ventral horn (Chen et al., 2006). Varying levels of Etv1-dependency reflect the differential requirement for Etv1 in the development of distinct, muscle-specific, pSN subtypes.

NIH-PA Author Manuscript NIH-PA Author Manuscript NIH-PA Author Manuscript